Bioorganic & Medicinal Chemistry 23 (2015) 5672–5680

Contents lists available at ScienceDirect

Bioorganic & Medicinal Chemistry

journal homepage: www.elsevier.com/locate/bmc

Antiproliferative and apoptosis-inducing activities of novel naphthalimide–cyclam conjugates through dual topoisomerase (topo) I/II inhibition

Shaoying Tan [†], Deheng Sun [†], Jiankun Lyu [†], Xiao Sun, Fangshu Wu, Qiang Li, Yiqi Yang, Jianxu Liu, Xin Wang, Zhuo Chen [*], Honglin Li [*], Xuhong Qian, Yufang Xu [*]

State Key Laboratory of Bioreactor Engineering, Shanghai Key Laboratory of New Drug Design, Shanghai Key Laboratory of Chemical Biology, School of Pharmacy, East China University of Science and Technology, Shanghai 200237, China

ARTICLE INFO

Article history:
Received 29 May 2015
Revised 8 July 2015
Accepted 9 July 2015
Available online 15 July 2015

Keywords:
Naphthalimide–cyclam conjugates
Antitumor agents
Topoisomerase I
Topoisomerase II
DNA intercalation
Apoptosis

ABSTRACT

A novel series of naphthalimide–cyclam conjugates were designed and synthesized. Among them, compounds **4c**, **4d**, **8c** and **8d** which bearing long lipophilic alkyl chains, displayed comparable or more potent cytotoxic activities against human tumor cell lines than amonafide. Furthermore, the four compounds were proved to possess strong inhibition against both topoisomerase I and II. The representative compound **8c** exhibited moderate DNA intercalation activity. Molecular modeling studies identified the possible interaction of compound **8c** with the molecular target by forming topoisomerase/DNA/drug ternary complex. Finally, derivatives with long lipophilic alkyl chains could efficiently induce apoptosis.

1. Introduction

Cancers, which figure among the leading causes of death worldwide, account for 8.2 million deaths in 2012, and a proposed rise to 13.1 million deaths in 2030.[1,2] Developing new anticancer drugs is an important goal of research nowadays. DNA targeted antitumor agents act as a mainstay of cancer chemotherapeutic agents by forming covalent complexes and/or declining in the function of DNA-processing enzymes.[3–5] DNA topoisomerases are omnipresent nuclear enzymes as active participant in the topological rearrangement of DNA during cellular processes like replication and transcription.[6] Topo I and topo II are the two main types of topoisomerases. Both of them could relax DNA supercoiling through a cleavage/relegation mechanism, only that topo I generates DNA single strand breaks and topo II breaks both strands of DNA.[7] Topoisomerases are over-expressed in cancer cells. To interfere with the enzymes or generate enzyme-mediated damages are clinically significant strategy in anticancer therapy.

Inhibition of topoisomerases could be classified by two categories: one is topoisomerase poisons which stabilizing the DNA–enzyme cleavable complex and causing an accumulation of broken DNA in the cell.[8] Most of these agents possess the structure components of a planar aromatic scaffold and a hydrogen bond donor side chain. Catalytic inhibitors, on the other hands, block the enzyme pocket before DNA cleavage or inhibit any steps of the catalytic cycle.[9–12] Compounds which modulate topo I or topo II specifically were used clinically in the treatment of various cancers. For example, camptothecin (CPT) analogues (topotecan and irinotecan) as topo I poisons and anthracycline derivatives (daunorubicin and doxorubicin) which inhibits topo II. New research also found that topo II were promising therapeutic target for the treatment of colon cancers with defective decatenation checkpoint.[13] However, it is found that selective topo I inhibition can induce a concomitant rise in the level of topo II expression, and vice versa. This phenomenon would lead to drug resistance and failure of clinical therapies ultimately. In this regard, compounds which have the potential to simultaneously inhibit topoisomerase I and II attracted great attention to improve antitumor activities and to overcome drug resistance problem.[8,14–17]

Macrocyclic derivatives, especially tetraazamacrocycles are applied in medical use. Cyclam (1,4,8,11-tetraazamacrocycle) is one of the most important members in the tetraazamacrocycles

* Corresponding authors. Tel./fax: +86 21 64250823 (Z.C.).
E-mail addresses: chenzhuo@ecust.edu.cn (Z. Chen), hlli@ecust.edu.cn (H. Li), yfxu@ecust.edu.cn (Y. Xu).
† These authors contributed equally to this work.

http://dx.doi.org/10.1016/j.bmc.2015.07.011
0968-0896/

family.[18,19] Normally, the medical use of tetraazamacrocycles is owing to their characters of binding various transition metal ions with high kinetic and thermodynamic stability.[20–22] Metal ion complexes of cyclam are applied in diagnosis and the treatment of AIDs.[19] Recently, cyclam–metal ion complexes were reported of their antitumor activities. Furthermore, introduction of lipophilic substitution were proved to be able to improve the ability of antiporliferative activity.[23,24] According to Sibert et al., two new lipophilic cyclam derivatives exhibited potent cytotoxic activity with IC_{50} values below 10 μM against cancer cell line L1210.[23]

Naphthalimide antitumor agents normally possess structural features of DNA intercalators, namely a flat aromatic or heteroaromatic moiety and basic side chains.[25] As shown in Figure 1, amonafide, which is the most famous one of them, could intercalate into DNA and strongly inhibited topo II. Amonafide reenters phase III clinical trial against secondary acute myeloid leukemia recently.[26] Herein, due to the antitumor potency of azomacrocycles, cyclam were introduced at the 2- or 6-position of naphthalimide core instead of flexible basic side chain. Besides, lipophilic long alkyl chains were introduced to naphthalimide–cyclam conjugates in comparison with methyl and butyl substitution (see Fig. 1). The newly-synthesized compounds were evaluated of their antiproliferative activity against solid tumor cell lines compared with amonafide and cyclam. Representative compounds were evaluated of their topo II/I inhibitory, DNA intercalation and collectively apoptosis inducing activity.

2. Chemistry

The target molecules **4a–4d** were synthesized in four steps from 6-bromobenzo[*de*]isochromene-1,3-dione as shown in Scheme 1. Firstly, the 6-bromobenzo[*de*]isochromene-1,3-dione was refluxed in ethanol with corresponding primary amine to obtain **1a–1d**. Then, **1a–1d** reacted with ethanol amine under Ullmann's condition to get **2a–2d**, which further converted to **3a–3d** in the existence of 2,3-dichloro-5,6-dicyano-benzoquinone (DDQ), tetrabutyl ammonium bromide and triphenylphosphine. Then the target molecules **4a–4d** were finally obtained by cyclam condensed with **3a–3d** in $CHCl_3$. **8a–8d** were synthesized in a similar process with **4a–4d** as shown in Scheme 2.

3. Results and discussions

3.1. In vitro cytotoxic activity

The antiproliferative activity of compounds **4a–4d**, **8a–8b** were evaluated against human cancer cell lines A549 (human non-small cell lung tumor cell), HeLa (human cervical carcinoma cell line), and HCT116 (human colon cancer cell line). Amonafide and cyclam were tested as reference compounds.

As show in the Table 1, all of the synthesized compounds displayed better antiporliferative than cyclam. Compounds **4c–4d**, **8c–8d** exhibited comparable or even more potent antiproliferative

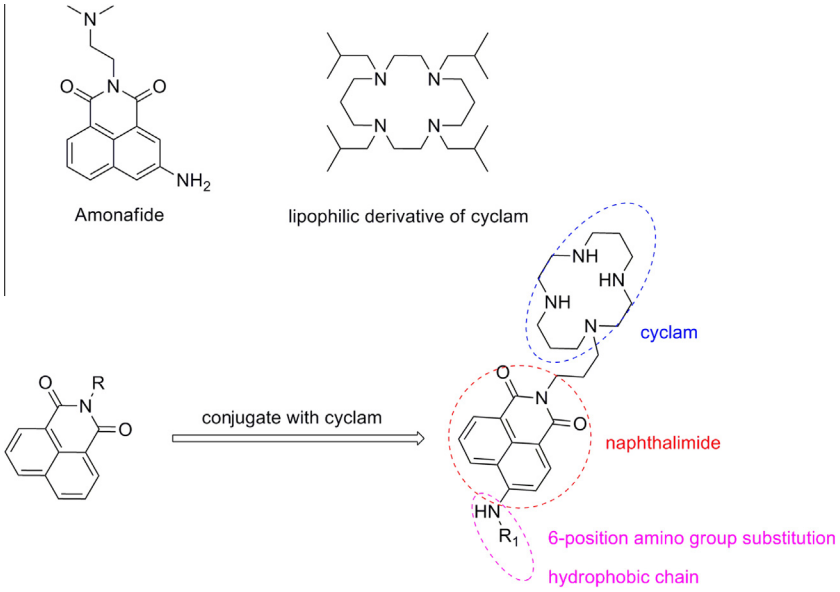

Figure 1. Structure of cyclam, amonafide and the design strategy of naphthalimide–cyclam conjugates.

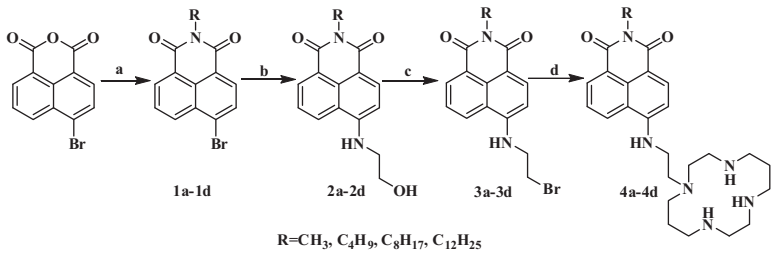

Scheme 1. Syntheses of target compounds **4a–4d**. (a) Corresponding primary amines, ethanol, reflux, 3 h; (b) ethanol amine, methoxyethanol, reflux, 4 h; (c) DDQ, PPh_3, $(n\text{-butyl})_4NBr$, CH_2Cl_2, rt, 12 h; (d) cyclam, KI, $CHCl_3$, rt, 72 h.

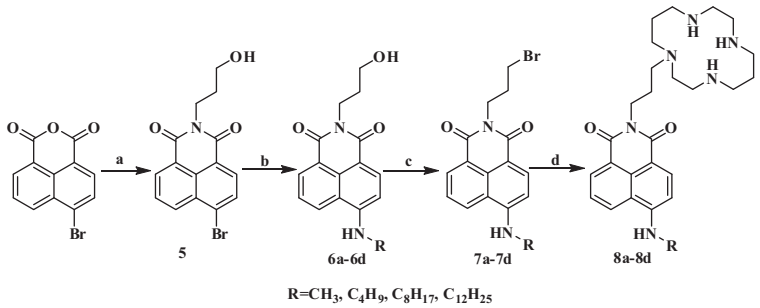

Scheme 2. Syntheses of target compounds **8a–8d**. (a) *n*-Propylamine, ethanol, reflux, 3 h; (b) corresponding primary amines, methoxyethanol, reflux, 4 h; (c) DDQ, PPh_3, $(n\text{-butyl})_4NBr$, CH_2Cl_2, rt, 12 h; (d) cyclam, KI, $CHCl_3$, rt, 72 h.

Table 1
SAR of cyclam fused naphthalimides

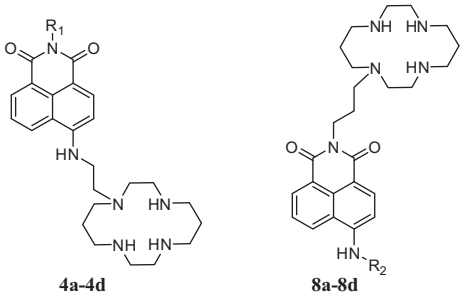

Compd	R, X=	Cytotoxicity[a] (IC_{50}, μM)		
		A549	HeLa	HCT116
4a	R_1 = $-CH_3$,	34.33 ± 2.04	13.80 ± 2.47	34.12 ± 2.47
4b	R_1 = *n*-C_4H_9,	38.89 ± 4.50	19.22 ± 0.20	29.22 ± 3.64
4c	R_1 = *n*-C_8H_{17}	15.77 ± 2.47	10.14 ± 2.51	16.73 ± 0.20
4d	R_1 = *n*-$C_{12}H_{25}$	18.41 ± 6.71	11.85 ± 4.00	18.18 ± 0.80
8a	R_2 = $-CH_3$,	>50	>50	>50
8b	R_2 = *n*-C_4H_9	>50	>50	>50
8c	R_2 = *n*-C_8H_{17}	11.58 ± 4.40	8.40 ± 2.62	8.07 ± 1.05
8d	R_2 = *n*-$C_{12}H_{25}$	15.84 ± 7.52	9.36 ± 1.85	13.00 ± 3.82
Cyclam		>50	>50	>50
Amonafide		n.d.[b]	9.52 ± 1.27	n.d.

[a] Cytotoxicity (CTX) against all of the human cancer cell were measured by sulforhodamine B dye-staining method.
[b] Not determined.

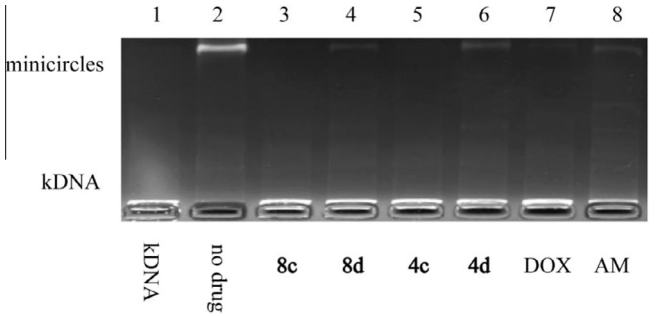

Figure 2. Inhibition of topo II-mediated kDNA decatenation by target compounds (100 μM). Lane 1, kDNA; lane 2, minicircles (no drug); lanes 3–8, compounds **8c**, **8d**, **4c**, **4d**, doxorubicin and amonafide, respectively.

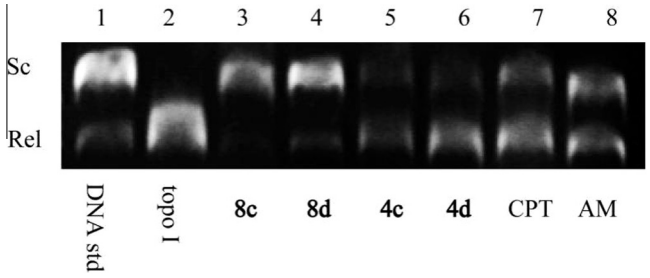

Figure 3. Inhibition of topo I-mediated DNA std (pBR322) decatenation by target compounds (100 μM except for CPT 200 μM). Lane 1, DNA std; lane 2, topo I (no drug); lanes 3–8, compounds **8c**, **8d**, **4c**, **4d**, camptothecin (CPT) and amonafide, respectively.

activity than amonafide, which stand for the rationale of naphthalimide–cyclam conjugates. Besides, introduction of long alkyl chain could improve the cytotoxic activity. For example, **8c** and **8d** was 4–6 fold more potent than **8a** and **8b** on HeLa and HCT116.

3.2. Effect on topoisomerases

According to previous report, amonafide, the most active naphthalimide antitumor derivative in clinical trial could intercalate into DNA and form a stable complex of drug–DNA–topoisomerase II. Since the newly-synthesized compounds also have similar structure feature of amonafide by containing a flat aromatic moiety and basic side chain, they were tested of their topo II inhibition activities with kinetoplast DNA (kDNA) assay.

As shown in Figure 2, decatenation kDNA by topo II were observed in lane 2. Addition of topo II inhibitor, such as doxorubicin (lane 7), would decrease the amount of released decatenated kDNA minicircles. Compounds **8d** and **4d** showed similar topo II inhibition activity as amonafide. Furthermore, compounds **8c** and **4c** were more potent than amonafide. This result were in accordance with the antiproliferation activity tendency that derivatives with octyl chain (**8c** and **4c**) were more potent than dodecyl derivative (**8c** vs **8d**, and **4c** vs **4d**). However, no obvious difference on topo II inhibition were observed between compounds **8** and compounds **4**. Therefore, other mechanism of action was supposed to exist due to the advantages of compounds **8c** and **8d** than **4c** and **4d** on their antiporliferative properties.

Due to the similar mechanism of topo I and II by relaxation of DNA supercoiling, we tested the target compounds if they could also affect topoisomerase I. According to Figure 3, compounds **4c** and **4d** could inhibit topo I activity less potent than the reference compounds camptothecin and amonafide. What's more, compounds **8c** and **8d**, were more efficient topo I inhibitors than camptothecin and amonafide. This result matched the cytotoxic activities that compound **8** were more potent than the corresponding compound **4** analogues. (**8c** vs **4c**, and **8d** vs **4d**).

3.3. DNA intercalating studies by circular dichroism (CD) spectra

Furthermore, the most active compound **8c** were confirmed of its DNA intercalation activity by CD spectra as intercalating agents could induce calf thymus DNA's (ctDNA) conformation changes. In accordance with literature, amonafide could induce significant changes in a negative peak around 245 nm and a positive peak around 275 nm due to helical B conformation and base stacking, respectively (see Fig. 4). Compound **8c** could also induce weaker conformational changes in comparison with amonafide. Therefore, compound **8c** was moderate DNA intercalator.

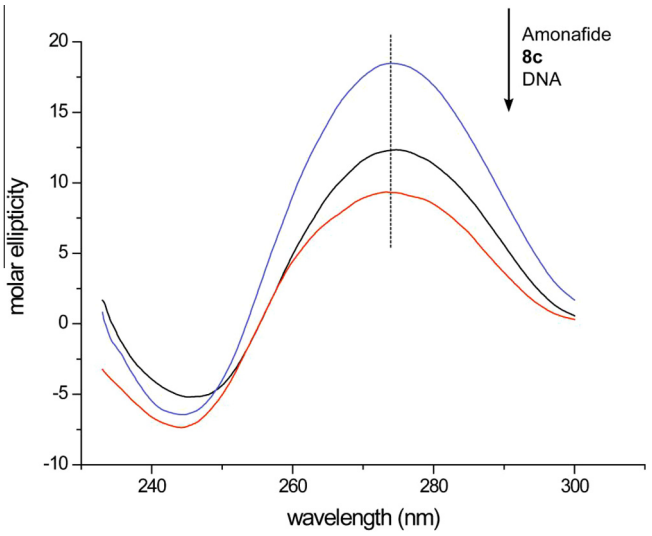

Figure 4. CD spectra of CT DNA (100 μM) incubated with representative compound **8c** (20 μM).

3.4. Molecular modeling

To better understand the molecular basis for the inhibition of topoisomerases induced by this series of compounds, molecular docking was adopted to predict the binding modes of the representative compound **8c**. The structures of the complex topoisomerase I/DNA/topotecan (PDB ID: 1K4T) and of the complex topoisomerase II/DNA/mitoxantrone (PDB ID: 4G0V) were used as receptor during the respective simulation. The lowest-energy poses predicted by Glide software are shown in Figure 5.

In both binding modes proposed by docking simulations, the nucleus of compound **8c** was intercalated at the site of double strand DNA cleavage and formed base-stacking interactions with base pairs upstream and downstream. In the case of enzyme topoisomerase I (Fig. 5A and B), compound **8c** interacted with nearby ASP533 and ARG364 residues, forming two H-bonds, respectively. Particularly, the carbonyl oxygen of the scaffold established an H-bond with the side chain of arginine, while the other H-bond was between the nitrogen atom of cyclam ring and the carboxylate ion of aspartate. In contrast, the case of topoisomerase II (Fig. 5C and D), compound **8c** formed multiple H-bonds with both enzyme and DNA. The carbonyl oxygens on the scaffold were contacted with DNA base pairs and GLN778 residue. The alkane side chain established an H-bond with the backbone oxygen atom of

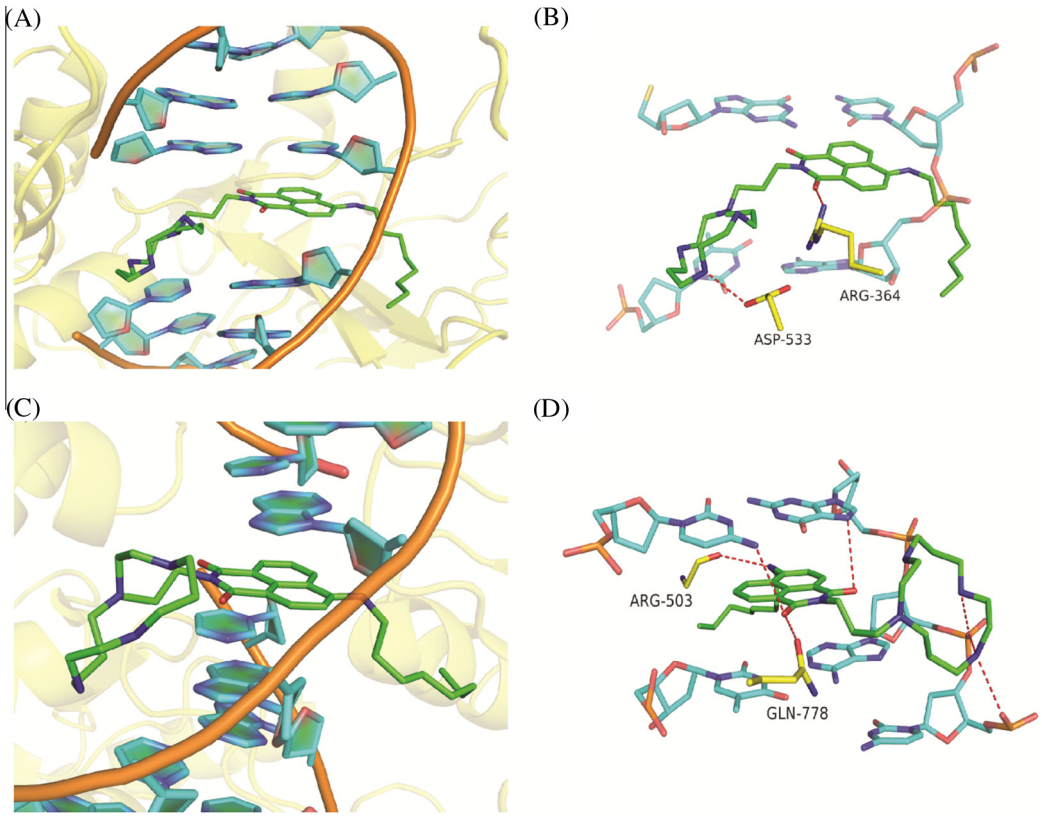

Figure 5. The binding poses for the compound **8c**. (A) docking model with the topo I/DNA complex; (B) binding mode with contacting residues and base pairs of topo I/DNA complex; (C) docking model with the topo II/DNA complex; (D) binding mode with contacting residues and base pairs of topo II/DNA complex. In docking models, the enzymes are depicted as transparent cartoons. In binding modes, the non-contact parts of enzyme and DNA are hidden for clarity, whereas the residues of DNA and enzyme are reported in different colored sticks. In all the cases, the H-bonds are highlight as red dashes, the compound is shown as green carbon colored sticks.

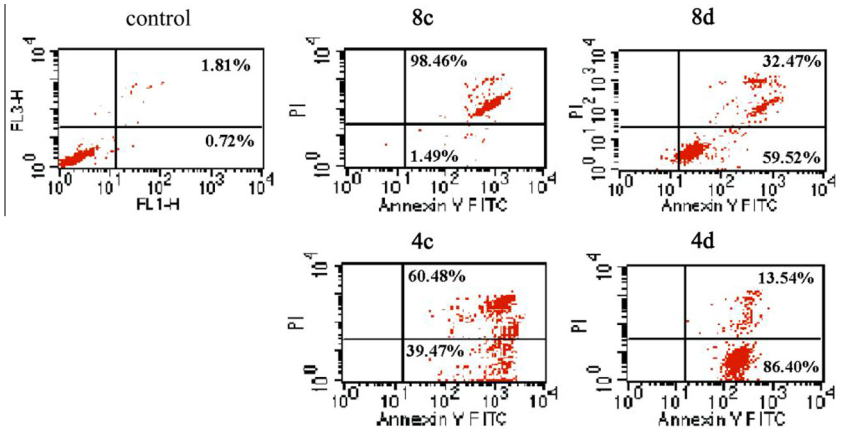

Figure 6. Apoptotic cells were detected with Annexin V/PI double staining after incubation with compound **8c**–**8d** and **4c**–**4d** for 24 h.

ARG503, as well as, the cyclam ring interacted with the backbone polar atoms of DNA strand.

3.5. Apoptosis assay by Annexin V binding

As DNA intercalation and topoisomerase poison could induce apoptosis in cancer cell lines, an Annexin V/PI assay was used to quantitate the apoptotic cells of HeLa induced by compounds with antitumor potency (compounds **4c**, **4d** and **8c**, **8d**). As illustrated in Figure 6, all the tested compounds could efficiently induce apoptosis of Hela cells at the concentration of 10 μM. After incubated for 24 h, compounds **8c** and **4c** induce the majority of HeLa cells into the late apoptotic stage (98.46%, 60.48%, respectively), while compound **8d** and **4d** induced the major amount of HeLa cells into the early apoptotic stage (59.52%, 86.40%, respectively). In all, all the tested compounds induce more than 90% apoptosis of HeLa cells.

4. Conclusion

In this paper, a series of naphthalimide–cyclam conjugates were designed and synthesized. The novel compounds could inhibit the growth of cancer cell lines comparable or even more potent than amonafide. Representative compounds **8c**, **8d**, **4c**, **4d** were investigated of their antitumor mechanism of action. They could potently inhibit both topo II and topo I in cell-free system. We also chose the most active compound **8c** and confirmed of its DNA intercalation activity. The molecular interactions between **8c** and its intracellular targets were investigated by molecular modeling simulations. Finally, the inhibition of HeLa cell growth by representative compounds **8c**, **8d**, **4c**, **4d** were associated with induction of apoptosis.

5. Experimental section

All the chemical regents and solvents were analytic grade. All the synthesized cyclam fused naphthalimide derivatives were verified by ^{1}H NMR, ^{13}C NMR and HRMS, while the metal complexes were verified by HRMS and HPLC. ^{1}H NMR and ^{13}C NMR measured on a Bruker AV-400 spectrometer (in $CDCl_3$ and DMSO-d_6, TMS as an internal standard). HRMS were collected in the Center of Analysis & Test of East China University of Science and Technology. Analytical HPLC was performed on a Hewlett-Packard 1100 system chromatograph equipped with photodiode array detector. Amonafide and camptothecin were purchased from Selleck chemicals (Houston, TX, USA). All medium and FBS were purchased from Gibco (Grand Island, NY, USA).

5.1. Synthesis

5.1.1. General procedure for the preparation of 1a–1d

6-Bromobenzo[*de*]-isochromene-1,3-dione (1.94 g, 7.00 mmol) was dissolved in 20 ml ethanol. Then corresponding primary amine (7.70 mmol) was added, and the mixture was stirred at 60 °C for 5–6 h. The mixture was cooled to room temperature and evaporated in vacuum to obtain the residue. Then the residue was purified on silica gel chromatography (PE:EA = 10:1, V/V) to provide **1a**–**1d**.

5.1.1.1. 6-Bromo-2-methyl-1*H*-benzo[*de*]isoquinoline-1,3(2*H*)-dione (1a). White solid, yield: 90%. ^{1}H NMR (400 MHz, $CDCl_3$): δ 8.68 (d, J = 7.2 Hz, 1H), 8.59 (d, J = 8.4 Hz, 1H), 8.44 (d, J = 8.0 Hz, 1H), 8.06 (d, J = 7.6 Hz, 1H), 7.86 (t, J = 8.4 Hz, 1H), 3.57 (s, 3H); MS(ESI) calcd for $C_{13}H_9BrNO_2$ $[M+H]^+$ 289.0, found: 289.0.

5.1.1.2. 6-Bromo-2-butyl-1*H*-benzo[*de*]isoquinoline-1,3(2*H*)-dione (1b). White solid, yield: 80%. ^{1}H NMR (400 MHz, $CDCl_3$) δ 8.66 (d, J = 7.2 Hz, 1H), 8.56 (d, J = 8.8 Hz, 1H), 8.41 (d, J = 8.0 Hz, 1H), 8.04 (d, J = 8.0 Hz, 1H), 7.85 (t, J = 8.0 Hz, 1H), 4.19 (t, J = 7.6 Hz, 1H), 1.77–1.69 (m, 2H), 1.51–1.42 (m, 2H), 1.00 (t, J = 7.2 Hz, 3H); MS(ESI) calcd for $C_{16}H_{15}BrNO_2$ $[M+H]^+$ 331.0, found: 331.0.

5.1.1.3. 6-Bromo-2-octyl-1*H*-benzo[*de*]isoquinoline-1,3(2*H*)-dione (1c). White solid, yield: 85%. ^{1}H NMR (400 MHz, $CDCl_3$): δ 8.68 (d, J = 7.2 Hz, 1H), 8.59 (d, J = 7.6 Hz, 1H), 8.44 (d, J = 8.0 Hz, 1H), 8.06 (d, J = 8.0 Hz, 1H), 7.87 (t, J = 7.6 Hz, 1H), 4.18 (t, J = 8.0 Hz, 2H), 1.78–1.71 (m, 2H), 1.47–1.29 (m, 10H), 0.89 (t, J = 7.2 Hz, 3H); MS(ESI) calcd for $C_{20}H_{23}BrNO_2$ $[M+H]^+$ 387.1, found: 387.1.

5.1.1.4. 6-Bromo-2-dodecyl-1*H*-benzo[*de*]isoquinoline-1,3(2*H*)-dione (1d). White solid, yield: 85%. ^{1}H NMR (400 MHz, $CDCl_3$): δ 8.68 (d, J = 7.2 Hz, 1H), 8.59 (d, J = 8.4 Hz, 1H), 8.44 (d, J = 7.6 Hz, 1H), 8.06 (d, J = 8.0 Hz, 1H), 7.87 (t, J = 7.6 Hz, 1H), 4.18 (t, J = 7.6 Hz, 2H), 1.78–1.71 (m, 2H), 1.47–1.27 (m, 18H), 0.90 (t, J = 7.2 Hz, 3H); MS(ESI) calcd for $C_{24}H_{31}BrNO_2$ $[M+H]^+$ 443.1, found: 443.2.

5.1.2. General procedure for the preparation of 2a–2d

1a–**1d** (6 mmol) were dissolved in 50 ml 2-methoxyethanol, respectively. Then ethanolamine (24 mmol) was added and the mixture was refluxed for 6 h. 150 ml water was added and solid

was precipitated immediately. The crude production was obtained by suction filtration and was purified on silica gel chromatography (CH_2Cl_2/MeOH = 50:1–20:1, V/V).

5.1.2.1. 6-(2-Hydroxyethylamino)-2-methyl-1*H*-benzo[*de*]isoquinoline-1,3(2*H*)-dione (2a). Yellow solid, yield: 90%. ^{1}H NMR (400 MHz, DMSO-d_6): δ 8.68 (d, J = 8.4 Hz, 1H), 8.43 (d, J = 7.2 Hz, 1H), 8.25 (d, J = 8.8 Hz, 1H), 7.67 (t, J = 8.0 Hz, 1H), 6.81 (d, J = 8.4 Hz, 1H), 3.69 (t, J = 6.0, 2H), 3.46 (t, J = 6.0, 2H); MS(ESI) calcd for $C_{15}H_{15}N_2O_3$ $[M+H]^+$ 270.1, found: 270.1.

5.1.2.2. 6-(2-Hydroxyethylamino)-2-butyl-1*H*-benzo[*de*]isoquinoline-1,3(2*H*)-dione (2b). Yellow solid, yield: 87%. ^{1}H NMR (400 MHz, $CDCl_3$): δ 8.58 (d, J = 7.2 Hz, 1H), 8.46 (d, J = 8.4 Hz, 1H), 8.16 (d, J = 8.4 Hz, 1H), 7.64 (t, J = 8.4 Hz, 1H), 6.79 (d, J = 8.4 Hz, 1H), 4.17 (t, J = 7.6 Hz, 2H), 4.09 (t, J = 5.2 Hz, 2H), 3.60 (t, J = 5.2 Hz, 1H), 1.74–1.70 (m, 2H), 1.49–1.43 (m, 2H), 0.99 (t, J = 7.6 Hz, 3H). MS(ESI) calcd for $C_{18}H_{21}N_2O_3$ $[M+H]^+$ 312.1, found: 312.1.

5.1.2.3. 6-(2-Hydroxyethylamino)-2-octyl-1*H*-benzo[*de*]isoquinoline-1,3(2*H*)-dione (2c). Yellow solid, yield: 84%. ^{1}H NMR (400 MHz, $CDCl_3$): δ 8.57 (d, J = 7.2 Hz, 1H), 8.45 (d, J = 8.4 Hz, 1H), 8.13 (d, J = 8.4 Hz, 1H), 7.62 (t, J = 7.6 Hz, 1H), 6.74 (d, J = 8.4 Hz, 1H), 4.16 (t, J = 8.0 Hz, 2H), 4.09 (t, J = 5.2 Hz, 2H), 3.60 (t, J = 5.2 Hz, 2H), 1.77–1.70 (m, 2H), 1.47–1.28 (m, 10H), 0.89 (t, J = 7.2 Hz, 3H); MS(ESI) calcd for $C_{22}H_{29}N_2O_3$ $[M+H]^+$ 369.2, found: 369.2.

5.1.2.4. 6-(2-Hydroxyethylamino)-2-dodecyl-1*H*-benzo[*de*]isoquinoline-1,3(2*H*)-dione (2d). Yellow solid, yield: 84%. ^{1}H NMR (400 MHz, $CDCl_3$): δ 8.53 (d, J = 7.2 Hz, 1H), 8.41(d, J = 8.4 Hz, 1H), 8.11 (d, J = 8.0 Hz, 1H), 7.59 (t, J = 8.0 Hz, 1H), 6.71 (d, J = 8.4 Hz, 1H), 4.15 (t, J = 7.6 Hz, 2H), 4.09 (t, J = 5.2 Hz, 2H), 3.58 (t, J = 5.2 Hz, 2H), 1.76–1.69 (m, 2H), 1.45–1.26 (m, 18H), 0.89 (t, J = 7.2 Hz, 3H); MS(ESI) calcd for $C_{26}H_{37}N_2O_3$ $[M+H]^+$ 425.3, found: 425.3.

5.1.3. General procedure for the preparation of 3a–3d

2,3-Dichloro-5,6-dicyano-1,4-benzoquinone (0.41 g, 1.80 mmol) and triphenyl phosphine (0.47 g, 1.80 mmol) were dissolved in 10 ml dry $CHCl_3$. Then the mixture of tetrabutyl ammonium bromide (0.58g, 1.80 mmol), **2a**–**2d** (1.50 mmol, respectively) and 10 ml dry $CHCl_3$ was dropped. 6 h later, the solvent was concentrated by vacuum and **3a**–**3d** were purified on silica gel chromatography (CH_2Cl_2).

5.1.3.1. 6-((2-Bromoethyl)amino)-2-methy-1*H*-benzo[*de*]isoquinoline-1,3(2*H*)-dione (3a). Orange solid, yield: 75%. ^{1}H NMR (500 MHz, $CDCl_3$): δ 8.63 (d, J = 7.3 Hz, 1H), 8.50 (d, J = 7.2 Hz, 1H), 8.15 (d, J = 8.3 Hz, 1H), 7.69 (t, J = 8.0 Hz, 1H), 6.75 (d, J = 6.9 Hz, 1H), 3.89 (t, J = 5.8 Hz, 2H), 3.76 (t, J = 5.7 Hz, 2H), 3.54 (s, 3H); MS(ESI) calcd for $C_{15}H_{14}BrN_2O_2$ $[M+H]^+$ 332.0, found: 332.0.

5.1.3.2. 6-((2-Bromoethyl)amino)-2-butyl-1*H*-benzo[*de*]isoquinoline-1,3(2*H*)-dione (3b). Orange solid, yield: 68%. ^{1}H NMR (400 MHz, $CDCl_3$): δ 8.62 (d, J = 7.2 Hz, 1H), 8.49 (d, J = 8.4 Hz, 1H), 8.15 (d, J = 8.4 Hz, 1H), 7.68 (t, J = 7.6 Hz, 1H), 6.76 (d, J = 8.4 Hz, 1H), 4.18 (t, J = 7.6 Hz, 2H), 3.89 (t, J = 6.0 Hz, 2H), 3.77 (t, J = 6.0 Hz, 1H), 1.77–1.69 (m, 2H), 1.51–1.41 (m, 2H), 0.99 (t, J = 7.2 Hz, 3H). MS (ESI) calcd for $C_{18}H_{20}BrN_2O_2$ $[M+H]^+$ 375.1, found: 375.0.

5.1.3.3. 6-((2-Bromoethyl)amino)-2-octyl-1*H*-benzo[*de*]isoquinoline-1,3(2*H*)-dione (3c). Orange solid, yield: 85%. ^{1}H NMR (400 MHz, $CDCl_3$): δ 8.63 (d, J = 6.4 Hz, 1H), 8.50 (d, J = 8.4 Hz, 1H), 8.16 (d, J = 7.6 Hz, 1H), 7.69 (t, J = 8.0 Hz, 1H), 6.77 (d, J = 8.4 Hz, 1H), 5.60 (br, 1H), 4.17 (t, J = 7.6 Hz, 2H), 3.89 (q, J = 4.4 Hz, 2H), 3.77 (t, J = 6.0 Hz, 2H), 1.78–1.70 (m, 2H), 1.47–1.28 (m, 10H), 0.89 (t, J = 7.2 Hz, 3H); MS(ESI) calcd for $C_{22}H_{28}BrN_2O_2$ $[M+H]^+$ 431.1, found: 431.1.

5.1.3.4. 6-((2-Bromoethyl)amino)-2-dodecyl-1*H*-benzo[*de*]isoquinoline-1,3(2*H*)-dione (3d). Orange solid, yield: 83%. ^{1}H NMR (400 MHz, $CDCl_3$): δ 8.63 (d, J = 7.2 Hz, 1H), 8.50 (d, J = 8.4 Hz, 1H), 8.16 (d, J = 8.0 Hz, 1H), 7.69 (t, J = 8.4 Hz, 1H), 6.77 (d, J = 8.4 Hz, 1H), 5.60 (br, 1H), 4.17 (t, J = 7.6 Hz, 2H), 3.89 (t, J = 5.6 Hz, 2H), 3.77 (t, J = 6.0 Hz, 2H), 1.78–1.70 (m, 2H), 1.45–1.27 (m, 18H), 0.90 (t, J = 7.2 Hz, 3H), MS(ESI) calcd for $C_{26}H_{36}BrN_2O_2$ $[M+H]^+$ 487.2, found: 487.2.

5.1.4. General procedure for the preparation of 4a–4d

1,4,8,11-Tetraazacyclotetradecane (0.10 g, 0.50 mmol) was dissolved in 10 ml dry $CHCl_3$. Then the mixture of **3a**–**3d** (0.20 mmol, respectively) and 15 ml dry $CHCl_3$ was dropped in rt under the argon. 3 days later, the solvent was concentrated by vacuum and **4a**–**4d** was purified on silica gel chromatography (CH_2Cl_2/MeOH/ammonium hydroxide = 100:15:2).

5.1.4.1. 6-((2-(1,4,8,11-Tetraazacyclotetradecan-1-yl)ethyl)amino)-2-methyl-1*H*-benzo[*de*]isoquinoline-1,3(2*H*)-dione (4a). Orange solid, yield: 50%. ^{1}H NMR (400 MHz, CD_3OD): δ 8.24–8.18 (m, 2H), 8.05 (d, J = 8.4 Hz, 1H), 7.40 (t, J = 8.4 Hz, 1H), 6.59 (d, J = 8.4 Hz, 1H), 3.50 (t, J = 7.2, 2H), 3.34 (s, 3H), 2.78–2.53 (m, 18H), 1.79–1.71 (m, 4H); ^{13}C NMR (100 MHz, CD_3OD): δ 164.9, 164.4, 150.9, 134.3, 130.7, 129.6, 127.8, 124.0, 121.8, 120.4, 107.9, 103.7, 54.4, 53.5, 50.7, 50.5, 49.2, 48.3, 46.7, 40.2, 27.4, 25.3, 24.1; HRMS (ESI) calcd for $C_{25}H_{37}N_6O_2$ $[M+H]^+$ 453.2978, found: 453.2968.

5.1.4.2. 6-((2-(1,4,8,11-Tetraazacyclotetradecan-1-yl)ethyl)amino)-2-butyl-1*H*-benzo[*de*]isoquinoline-1,3(2*H*)-dione (4b). Orange solid, yield: 66%. ^{1}H NMR (400 MHz, $CDCl_3$): δ 9.09 (d, J = 8.0 Hz, 1H), 8.58 (d, J = 6.8 Hz, 1H), 8.43 (d, J = 8.4 Hz, 1H), 7.80 (t, J = 6.0 Hz, 1H), 7.66 (t, J = 7.6 Hz, 1H), 6.68 (d, J = 8.8 Hz, 1H), 4.17 (t, J = 7.6 Hz, 2H), 3.79 (d, J = 5.6 Hz, 2H), 3.09–3.03 (m, 4H), 2.97 (br, 2H), 2.89 (br, 2H), 2.73 (t, J = 4.8 Hz, 2H), 1.77–1.69 (m, 2H), 1.49–1.43 (m, 2H), 0.98 (t, J = 7.2 Hz, 3H). ^{13}C NMR (100 MHz, $CDCl_3$): δ 164.8, 164.2, 150.4, 134.5, 131.3, 130.1, 128.9, 124.4, 122.8, 120.7, 109.2, 103.5, 51.2, 51.0, 50.8, 50.6, 47.2, 46.8, 46.4, 46.0, 45.1, 40.1, 40.0, 30.3, 25.8, 25.2, 20.5, 13.9; HRMS (ESI) calcd for $C_{28}H_{43}N_6O_2$ $[M+H]^+$ 495.3448, found: 495.3454.

5.1.4.3. 6-((2-(1,4,8,11-Tetraazacyclotetradecan-1-yl)ethyl)amino)-2-octyl-1*H*-benzo[*de*]isoquinoline-1,3(2*H*)-dione (4c). Orange solid, yield: 65%. ^{1}H NMR (400 MHz, CD_3OD): δ 8.31–8.28 (m, 2H), 8.16 (d, J = 8.4 Hz, 1H), 7.45 (t, J = 8.0 Hz, 1H), 6.66 (d, J = 8.8 Hz, 1H), 3.99 (t, J = 7.2 Hz, 2H), 3.50 (t, J = 6.4 Hz, 2H), 2.77–2.51 (m, 18H), 1.77–1.62 (m, 6H), 1.31–1.23 (m, 10H), 0.85 (t, J = 7.2 Hz, 3H); ^{13}C NMR (100 MHz, CD_3OD): δ 164.4, 163.8, 150.7, 134.3, 130.6, 129.6, 127.7, 123.9, 121.9, 120.3, 108.1, 103.6, 54.5, 53.7, 50.8, 50.6, 49.3, 48.5, 46.8, 40.3, 39.7, 31.6, 29.1, 29.1, 27.9, 27.6, 26.9, 25.4, 22.4, 13.2; HRMS (ESI) calcd for $C_{32}H_{51}N_6O_2$ $[M+H]^+$ 551.4074, found: 551.4070.

5.1.4.4. 6-((2-(1,4,8,11-Tetraazacyclotetradecan-1-yl)ethyl)amino)-2-dodecyl-1*H*-benzo[*de*]isoquinoline-1,3(2*H*)-dione (4d). Orange solid, yield: 62%. ^{1}H NMR (400 MHz, CD_3OD): δ 8.33–8.29 (m, 2H), 8.18 (d, J = 8.4 Hz, 1H), 7.47 (t, J = 8.0 Hz, 1H), 6.67 (d, J = 8.8 Hz, 1H), 4.00 (t, J = 7.2 Hz, 2H), 3.52 (t, J = 6.4 Hz, 2H), 2.78–2.53 (m, 18H), 1.77–1.63 (m, 6H), 1.31–1.19 (m, 18H), 0.85 (t, J = 7.2 Hz, 3H); ^{13}C NMR (100 MHz, CD_3OD): δ 164.4, 163.8, 150.7, 134.3, 130.6, 129.6, 127.8, 123.9, 121.9, 120.3, 108.1, 103.6, 54.5, 53.7, 50.8, 50.6, 49.3, 48.5, 46.8, 40.3, 39.7, 31.7, 29.4, 29.2, 29.2, 27.9, 27.5, 26.9, 25.4, 22.4, 13.3; HRMS (ESI) calcd for $C_{36}H_{59}N_6O_2[M+H]^+$ 607.4700, found: 607.4688.

5.1.5. 6-Bromo-2-(3-hydroxypropyl)-1*H*-benzo[*de*]isoquinoline-1,3(2*H*)-dione (5)

6-Bromobenzo[*de*]-isochromene-1,3-dione (1.94 g, 7.00 mmol) was dissolved in 20 ml ethanol. Then 3-amino-1-propanol (7.70 mmol) was added, and the mixture was refluxed for 5–6 h. The mixture was cooled to room temperature and evaporated in vacuum to obtain the residue. Then the residue was recrystallized by EtOH to obtained 5. White solid, yield: 90%. ^{1}H NMR (400 MHz, $CDCl_3$): δ 8.68 (d, J = 7.2 Hz, 1H), 8.60 (d, J = 8.0 Hz, 1H), 8.43 (d, J = 7.6 Hz, 1H), 8.07 (d, J = 8 Hz, 1H), 7.87 (t, J = 8.0 Hz, 2H), 4.36 (t, J = 6.0 Hz, 2H), 3.62 (t, J = 6.0 Hz, 2H), 2.63 (br, 1H), 2.04–1.98 (m, 2H); MS (EI) calcd for $C_{15}H_{12}BrNO_3$ [M^+] 333.0, found: 333.0.

5.1.6. General procedure for the preparation of 6a–6d

5 (2.0 g, 6 mmol) were dissolved in 50 ml 2-methoxyethanol. Then corresponded amines (24 mmol) was added and the mixture was refluxed for 6 h. 150 ml water was added and solid was precipitated immediately. The crude production was obtained by suction filtration and was purified on silica gel chromatography (CH_2Cl_2/MeOH = 50:1–20:1, V/V).

5.1.6.1. 2-(3-Hydroxypropyl)-6-(methylamino)-1*H*-benzo[*de*]-isoquinoline-1,3(2*H*)-dione (6a). Yellow solid, yield: 79%. ^{1}H NMR (400 MHz, $CDCl_3$): δ 8.63 (d, J = 8.4 Hz, 1H), 8.54 (d, J = 8.4 Hz, 1H), 8.14 (d, J = 8.4 Hz, 1H), 7.69 (t, J = 8.0 Hz, 1H), 6.79 (d, J = 8.0 Hz, 1H), 4.36 (t, J = 6.0 Hz, 2H), 3.58 (t, J = 5.6 Hz, 2H), 3.19 (s, 3H), 2.03–1.97 (m, 2H); MS (ESI) calcd for $C_{16}H_{17}N_2O_3$ $[M+H]^+$ 285.1, found: 285.1.

5.1.6.2. 2-(3-Hydroxypropyl)-6-(butylamino)-1*H*-benzo[*de*]isoquinoline-1,3(2*H*)-dione (6b). Yellow solid, yield: 87%. ^{1}H NMR (400 MHz, $CDCl_3$): δ 8.61 (d, J = 6.4 Hz, 1H), 8.50 (d, J = 8.4 Hz, 1H), 8.14 (d, J = 8.4 Hz, 1H), 7.66 (t, J = 7.6 Hz, 1H), 6.78 (d, J = 8.4 Hz, 1H), 4.36 (t, J = 6.0 Hz, 2H), 3.57 (t, J = 5.6 Hz, 2H), 3.45 (t, J = 7.2 Hz, 2H), 2.03–1.97 (m, 2H), 1.87–1.80 (m, 2H), 1.61–1.52 (m, 2H), 1.05 (t, J = 7.2 Hz, 3H); MS (ESI) calcd for $C_{19}H_{23}N_2O_3$ $[M+H]^+$ 285.1, found: 285.1.

5.1.6.3. 2-(3-Hydroxypropyl)-6-(octylamino)-1*H*-benzo[*de*]isoquinoline-1,3(2*H*)-dione (6c). Yellow solid, yield: 90%. ^{1}H NMR (400 MHz, $CDCl_3$): δ 8.62 (d, J = 8.0 Hz, 1H), 8.50 (d, J = 8.4 Hz, 1H), 8.13 (d, J = 8.0 Hz, 1H), 7.65 (t, J = 8.0 Hz, 1H), 6.75 (d, J = 8.4 Hz, 1H), 4.36 (t, J = 6.0 Hz, 2H), 3.57 (t, J = 5.6 Hz, 2H), 3.43 (t, J = 7.2 Hz, 2H), 2.02–1.97 (m, 2H), 1.87–1.80 (m, 2H), 1.56–1.32 (m, 10H), 0.91 (t, J = 6.8 Hz, 3H); MS (ESI) calcd for $C_{23}H_{31}N_2O_3$ $[M+H]^+$ 383.2, found: 383.2.

5.1.6.4. 2-(3-Hydroxypropyl)-6-(dodecylamino)-1*H*-benzo[*de*]-isoquinoline-1,3(2*H*)-dione (6d). Yellow solid, yield: 90%.^{1}H NMR (400 MHz, $CDCl_3$): δ 8.62 (d, J = 6.4 Hz, 1H), 8.50 (d, J = 8.4 Hz, 1H), 8.13 (d, J = 8.4 Hz, 1H), 7.66 (t, J = 8.0 Hz, 1H), 6.76 (d, J = 8.4 Hz, 1H), 4.36 (t, J = 6.0 Hz, 2H), 3.57 (t, J = 5.6 Hz, 2H), 3.44 (t, J = 7.2 Hz, 2H), 2.03–1.97 (m, 2H), 1.87–1.80 (m, 2H), 1.56–1.29 (m, 18H), 0.90 (t, J = 6.4 Hz, 3H); MS (ESI) calcd for $C_{27}H_{38}N_2O_3Na$ $[M+Na]^+$ 461.3, found: 461.3.

5.1.7. General procedure for the preparation of 7a–7d

2,3-Dichloro-5,6-dicyano-1,4-benzoquinone (0.41 g, 1.80 mmol) and triphenyl phosphine (0.47 g, 1.80 mmol) were dissolved in 10 ml dry $CHCl_3$. Then the mixture of tetrabutyl ammonium bromide (0.58 g, 1.80 mmol), **6a–6d** (1.50 mmol, respectively) and 10 ml dry $CHCl_3$ was dropped. 6 h later, the solvent was concentrated by vacuum and **7a–7d** were purified on silica gel chromatography (CH_2Cl_2).

5.1.7.1. 2-(3-Bromopropyl)-6-(methylamino)-1*H*-benzo[*de*]isoquinoline-1,3(2*H*)-dione (7a). Orange solid, yield: 73%. ^{1}H NMR (400 MHz, $CDCl_3$): δ 8.62 (d, J = 6.8 Hz, 1H), 8.53 (d, J = 8.4 Hz, 1H), 8.13 (d, J = 9.2 Hz, 1H), 7.67 (t, J = 8.4 Hz, 1H), 6.82–6.80 (m, 1H), 4.33 (t, J = 7.2 Hz, 2H), 3.52 (t, J = 6.8 Hz, 2H), 3.18 (s, 3H), 2.39–2.32 (m, 2H); MS (ESI) calcd for $C_{16}H_{14}BrN_2O_2$ $[M-H]^-$ 345.0, found: 345.0.

5.1.7.2. 2-(3-Bromopropyl)-6-(butylamino)-1*H*-benzo[*de*]isoquinoline-1,3(2*H*)-dione (7b). Orange solid, yield: 77%. ^{1}H NMR (400 MHz, $CDCl_3$): δ 8.58 (d, J = 7.2 Hz, 1H), 8.46 (d, J = 8.4 Hz, 1H), 8.11 (d, J = 8.4 Hz, 1H), 7.62 (t, J = 7.2 Hz, 1H), 6.73 (d, J = 8.0 Hz, 1H), 5.32 (br, 1H), 4.31 (t, J = 6.4 Hz, 2H), 3.52–3.49 (m, 2H), 3.45–3.41 (m, 2H), 2.37–2.31 (m, 2H), 1.86–1.79 (m, 2H), 1.60–1.51 (m, 2H), 1.04 (t, J = 7.6 Hz, 3H); MS (ESI) calcd for $C_{19}H_{20}BrN_2O_2$ $[M-H]^-$ 387.1, found: 387.1.

5.1.7.3. 2-(3-Bromopropyl)-6-(octylamino)-1*H*-benzo[*de*]isoquinoline-1,3(2*H*)-dione (7c). Orange solid, yield: 70%. ^{1}H NMR (400 MHz, $CDCl_3$): δ 8.60 (d, J = 7.2 Hz, 1H), 8.48 (d, J = 8.8 Hz, 1H), 8.11 (d, J = 8.4 Hz, 1H), 7.64 (t, J = 8.0 Hz, 1H), 6.74 (d, J = 8.4 Hz, 1H), 5.32 (br, 1H), 4.32 (t, J = 7.2 Hz, 2H), 3.51 (t, J = 7.2 Hz, 2H), 3.42 (t, J = 7.2 Hz, 2H), 2.38–2.31 (m, 2H), 1.87–1.80 (m, 2H), 1.55–1.32 (m, 10H), 0.91 (t, J = 6.8 Hz, 3H); MS (ESI) calcd for $C_{23}H_{30}BrN_2O_2$ $[M+H]^+$ 445.1, found: 445.1.

5.1.7.4. 2-(3-Bromopropyl)-6-(dodecylamino)-1*H*-benzo[*de*]isoquinoline-1,3(2*H*)-dione (7d). Orange solid, yield: 70%. ^{1}H NMR (400 MHz, $CDCl_3$): δ 8.60 (d, J = 7.6 Hz, 1H), 8.48 (d, J = 8.4 Hz, 1H), 8.11 (d, J = 8.0 Hz, 1H), 7.64 (t, J = 8.0 Hz, 1H), 6.75 (d, J = 8.4 Hz, 1H), 5.30 (br, 1H), 4.32 (t, J = 6.8 Hz, 2H), 3.51 (t, J = 7.2 Hz, 2H), 3.43 (t, J = 7.2 Hz, 2H), 2.38–2.31 (m, 2H), 1.87–1.80 (m, 2H), 1.55–1.29 (m, 18H), 0.90 (t, J = 6.8 Hz, 3H); MS (ESI) calcd for $C_{27}H_{37}N_2O_2$ $[M-Br]^+$ 421.3, found: 421.3.

5.1.8. General procedure for the preparation of 8a–8d

1,4,8,11-Tetraazacyclotetradecane (0.10 g, 0.50 mmol) was dissolved in 10 ml dry $CHCl_3$. Then the mixture of **7a–7d** (0.20 mmol, respectively) and 15 ml dry $CHCl_3$ was dropped in rt under the argon. 3 days later, the solvent was concentrated by vacuum and **8a–8d** was purified on silica gel chromatography (CH_2Cl_2/MeOH/ammonium hydroxide = 100:15:2).

5.1.8.1. 2-(3-(1,4,8,11-Tetraazacyclotetradecan-1-yl)propyl)-6-(methylamino)-1*H*-benzo[*de*]isoquinoline-1,3(2*H*)-dione (8a). Orange solid, yield: 47%. ^{1}H NMR (400 MHz, $CDCl_3$): δ 8.42 (d, J = 7.2 Hz, 1H), 8.31–8.28 (m, 2H), 7.49 (t, J = 8.0 Hz,1H), 6.50 (d, J = 8.4 Hz, 1H), 6.32 (br, 1H), 4.22 (t, J = 8.0 Hz, 2H), 3.15–3.10 (m, 5H), 2.94 (m, 10H), 2.76 (br, 2H), 2.64–2.58 (m, 4H), 1.98–1.91 (m, 6H); ^{13}C NMR (100 MHz, $CDCl_3$): δ 164.8, 164.1, 151.1, 134.5, 131.0, 129.5, 127.6, 124.2, 122.1, 120.2, 108.8, 103.5, 53.2, 52.5, 51.0, 50.7, 49.3, 48.3, 48.0, 46.9, 46.4, 38.5, 30.2, 25.8, 25.4, 24.9; HRMS (ESI) calcd for $C_{26}H_{38}N_6O_2Na$ $[M+Na]^+$ 489.2948, found: 489.2976.

5.1.8.2. 2-(3-(1,4,8,11-Tetraazacyclotetradecan-1-yl)propyl)-6-(butylamino)-1*H*-benzo[*de*]isoquinoline-1,3(2*H*)-dione (8b). Orange solid, yield: 52%. ^{1}H NMR (400 MHz, $CDCl_3$): δ 8.57 (d, J = 8.4 Hz, 1H), 8.00 (d, J = 7.2 Hz, 1H), 7.78 (d, J = 8.4 Hz, 1H), 7.25 (t, J = 8.0 Hz,1H), 6.20 (d, J = 8.8 Hz, 1H), 4.24 (br, 2H), 3.78 (br s, 2H), 3.60–3.31 (m, 10H), 3.03–2.80 (m, 6H), 2.25–2.16 (m, 4H), 1.88–1.79 (m, 4H), 1.54–1.45 (m, 4H), 1.00 (t, J = 7.6 Hz, 3H); ^{13}C NMR (100 MHz, $CDCl_3$): δ 164.8, 163.7, 151.4, 133.9, 130.7, 129.7, 129.3, 123.6, 120.4, 119.8, 106.6, 103.4, 54.2, 51.3, 51.2, 49.8, 48.6, 47.1, 44.7, 44.6, 43.2, 37.9, 30.5, 24.5, 23.7, 22.2, 20.5, 13.9; HRMS (ESI) calcd for $C_{29}H_{45}N_6O_2$ $[M+H]^+$ 509.3599, found: 509.3595.

5.1.8.3. 2-(3-(1,4,8,11-Tetraazacyclotetradecan-1-yl)propyl)-6-(octylamino)-1*H*-benzo[*de*]isoquinoline-1,3(2*H*)-dione (8c). Orange solid, yield: 55%. ^{1}H NMR (400 MHz, CD_3OD): δ 8.34–8.29 (m, 2H), 8.14 (d, J = 8.4 Hz, 1H), 7.46 (t, J = 8.0 Hz,1H), 6.54 (d, J = 8.8 Hz, 1H), 4.08 (t, J = 7.6 Hz, 2H), 3.33 (t, J = 6.8 Hz, 2H), 2.88–2.53 (m, 18H), 1.87–1.71 (m, 8H), 1.49–1.29 (m, 10H), 0.89 (t, J = 7.2 Hz, 3H); ^{13}C NMR (100 MHz, CD_3OD): δ 164.6, 163.9, 151.0, 134.3, 130.5, 129.6, 127.9, 123.8, 121.7, 120.2, 107.6, 103.4, 53.3, 53.0, 50.4, 50.1, 49.4, 46.8, 46.5, 43.2, 38.1, 31.7, 29.2, 29.1, 28.2, 27.0, 26.7, 24.9, 24.5, 22.4, 13.2; HRMS (ESI) calcd for $C_{33}H_{53}N_6O_2$ $[M+H]^+$ 565.4230, found: 565.4228.

5.1.8.4. 2-(3-(1,4,8,11-Tetraazacyclotetradecan-1-yl)propyl)-6-(dodecylamino)-1*H*-benzo[*de*]isoquinoline-1,3(2*H*)-dione (8d). Orange solid, yield: 58%. ^{1}H NMR (400 MHz, CD_3OD): δ 8.38–8.31 (m, 2H), 8.17 (d, J = 8.8 Hz, 1H), 7.50 (t, J = 8.0 Hz, 1H), 6.58 (d, J = 8.8 Hz, 1H), 4.10 (s, 2H), 3.35–3.33 (m, 2H), 2.89–2.54 (m, 18H), 1.85–1.78 (m, 8H), 1.46–1.24 (m, 18H), 0.88 (t, J = 7.2 Hz, 3H); ^{13}C NMR (100 MHz, CD_3OD): δ 164.6, 163.9, 151.1, 134.4, 130.6, 129.6, 127.9, 123.8, 121.7, 120.2, 107.6, 103.45, 53.4, 52.9, 50.4, 50.1, 49.4, 46.8, 46.4, 43.2, 38.1, 31.7, 29.4, 29.1, 28.2, 27.0, 26.6, 24.8, 24.5, 22.4, 13.2; HRMS (ESI) calcd for $C_{37}H_{61}N_6O_2$ $[M+H]^+$ 621.4856, found: 621.4857.

5.2. Cell lines and cell culture

HeLa was purchased from Cell Bank of Type Culture Collection of Chinese Academy of Sciences (Shanghai, China). A549 and HCT116 were purchased form American Type Culture Collection (ATCC, Manassas, VA, USA). They were maintained in strict accordance with the supplier's instructions and established procedures

5.3. In vitro cytotoxicity assays of the 4a–4d and 8a–8d

Cancer cells were seeded into 96-well plates and cultured overnight. The cells were then treated with increasing concentrations of compounds for a further 24 h. Cells were then fixed with 10% trichloroacetic acid and stained with sulforhodamine B (Sigma Aldrich, St. Louis, MO, USA). Sulforhodamine B in the cells was dissolved in 10 mM Tris–HCl and was measured at 515 nm using a multiwell spectrophotometer (MAX190™, Molecular Devices, Sunnyvale, USA). The inhibition rate on cell proliferation was calculated as follows: inhibition rate = $(1 - A_{515\ \text{treated}}/A_{515\ \text{control}}) \times 100\%$.

5.4. kDNA decatenation assay

Topoisomerase II activity was measured by the ATP-dependent decatenation of kDNA, which was provided by the manufacturer's instructions (TopoGEN, Florida, USA). 0.1 mg kDNA, 1 unit of human topo IIa (TopoGEN) and the corresponding concentrations of the measured compounds were incubated for 30 min at 37 °C in 50 mM TrisHCl (pH 8), 150 mM NaCl, 10 mM $MgCl_2$, 2 mM ATP, 0.5 mM DTT in a total volume of 20 μL. Then 2 μL 10% SDS and 2 μL 6× loading dye solution (Fermentas) were added to stop the reaction. Samples were then electrophoresed in 0.8% agarose gel in TAE buffer for 50 min at 120 V. The gel was stained with ethidium bromide at room temperature and photographed with UV transilluminator.

5.5. DNA relaxation assay

Topoisomerase I activity was assayed by relaxation of supercoiled pBR322 DNA according to the manufacturer's instructions (Takara, Dalian, China). TopoI (calf thymus), buffer, BSA, loading buffer and supercoiled pBR322 DNA were all from TaKaRa Biotechnology CO., Ltd 0.5 μg supercoiled pBR322 DNA, 0.1 units of topoisomerase I and the indicated concentrations of compounds were incubated for 30 min at 37 °C in DNA topoisomerase I buffer with 0.01% bovine serum albumin, in a total volume of 20 μL. The reactions were stopped by the addition of 2 μL 10% SDS and 2 μL 6× loading dye solution (Fermentas). Samples were then electrophoresed in 0.8% agarose gel in TAE buffer for 35 min at 120 V. The gel was stained with ethidium bromide at room temperature and photographed with UV transilluminator.

5.6. DNA intercalating assay by CD spectra

ct-DNA was purchased from Sigma Aldrich and used without further purification. A solution of ct-DNA in 20 mM Tris–HCl buffer (pH = 7.4) was stored at 4 °C. The concentration of ct-DNA was determined spectrophotometrically from the molar absorption coefficient (6600 M^{-1} cm^{-1}). The stock solution was attested to be sufficiently free from protein, as it gave a UV absorbance ratio at 260 and 280 nm of more than 1.8. The CD measurements were performed on a Chirascan spectrophotometer (Photophysics, England) using 1 cm quartz cell in the range of 200–400 nm. ct-DNA (100 μM) interacted with drugs (20 μM) in Tris–HCl buffer for 2 h at 25 °C. CD spectra in the range of 230–300 nm were analyzed.

5.7. Computational methods

The crystallographic structure of the complex topoisomerase I/DNA/topotecan (PDB ID: 1K4T) and of complex topoisomerase II/DNA/mitoxantrone (PDB ID: 4G0V) were fetched from Protein Data Bank (PDB, http://www.pdb.org). The protein/DNA/drug structures were prepared with protein preparation wizard in Maestro 9.0. Hydrogens were added and water molecules were deleted from the proteins. The final structures for following docking were minimized in Impref with OPLS-2005 force field. Compound **8c** was converted to 3D structure from 2D structure by LigPrep 2.3. The protonation state of the molecule was also assigned at physiological pH. Grids were automatically generated using Glide 5.5 with standard procedure recommended by Schrödinger. The centers of intercalation sites were defined by geometric centers of native ligands. Compound **8c** was docked using Glide in extra precision mode with default parameters. The docked poses discussed in this paper were selected accounting for both proper energy score and reasonable binding mode.

5.8. Annexin V-FIFC apoptosis detection assay

Annexin V-FITC apoptosis detection kit (Invitrogen, USA) was used in this assay. Briefly, HeLa cells (1×10^6/1.5 ml per well) were seeded in six-well plates and treated with the measured compounds at 10 μM. 24 h later, cells were treated with cold PBS, resuspended in 400 μL of binding buffer, and then added to 5 μL of annexin V-FITC, incubated at 4 °C in the dark for 15 min. Then

10 μL of PI was added and incubated same condition for 5 min. The samples were analyzed by a FACScan flow cytometer (Becton Dickinson, USA).

Acknowledgements

This work is financially supported by the Fundamental Research Funds for the Central Universities, the National Natural Science Foundation of China (Grants 21302054, 81222046, 21173076 and 81230076) (Z.C., H.L.), the Shanghai Committee of Science and Technology (Grants 14431902100, and 13ZR1453100) (Y.X., Z.C.), the Opening Fund of Shanghai Key Laboratory of Chemical Biology (Grant SKLCB-2012-05) (Z.C.), the National S&T Major Project of China (Grant 2013ZX09507004) and the 863 Hi-Tech Program of China (Grant 2012AA020308) (H.L.). H.L. is also sponsored by Shanghai Rising-Star Tracking Program (Grant 13QH1401100), Specialized Research Fund for the Doctoral Program of Higher Education (Grant 20130074110004) and Fok Ying Tung Education Foundation (Grant 141035).

References and notes

1. Lichtman, S. M. *Am. Soc. Clin. Oncol. Educ. Book* **2013**, 411.
2. Ferlay, J.; Soerjomataram, I.; Dikshit, R.; Eser, S.; Mathers, C.; Rebelo, M.; Parkin, D. M.; Forman, D.; Bray, F. *Int. J. Cancer* **2015**, *136*, E359.
3. Hurley, L. H. *Nat. Rev. Cancer* **2002**, *2*, 188.
4. Gurova, K. *Future Oncol.* **2009**, *5*, 1685.
5. Nitiss, J. L. *Nat. Rev. Cancer* **2009**, *9*, 338.
6. Champoux, J. J. *Annu. Rev. Biochem.* **2001**, *70*, 369.
7. Chen, A. Y.; Liu, L. F. *Annu. Rev. Pharmacol. Toxicol.* **1994**, *34*, 191.
8. Denny, W. A. *Expert Opin. Investig. Drugs* **1997**, *6*, 1845.
9. Pommier, Y.; Leo, E.; Zhang, H.; Marchand, C. *Chem. Biol.* **2010**, *17*, 421.
10. Akerman, K. J.; Fagenson, A. M.; Cyril, V.; Taylor, M.; Muller, M. T.; Akerman, M. P.; Munro, O. Q. *J. Am. Chem. Soc.* **2014**, *136*, 5670.
11. Kadayat, T. M.; Park, C.; Jun, K. Y.; Thapa Magar, T. B.; Bist, G.; Yoo, H. Y.; Kwon, Y.; Lee, E. S. *Eur. J. Med. Chem.* **2015**, *90*, 302.
12. Jun, K. Y.; Park, S. E.; Liang, J. L.; Jahng, Y.; Kwon, Y. *ChemMedChem* **2015**.
13. Jain, C. K.; Roychoudhury, S.; Majumder, H. K. *Biochim. Biophys. Acta* **1853**, *2015*, 1195.
14. Salerno, S.; Da Settimo, F.; Taliani, S.; Simorini, F.; La Motta, C.; Fornaciari, G.; Marini, A. M. *Curr. Med. Chem.* **2010**, *17*, 4270.
15. Denny, W. A.; Baguley, B. C. *Curr. Top. Med. Chem.* **2003**, *3*, 339.
16. Yao, B.-L.; Mai, Y.-W.; Chen, S.-B.; Xie, H.-T.; Yao, P.-F.; Ou, T.-M.; Tan, J.-H.; Wang, H.-G.; Li, D.; Huang, S.-L.; Gu, L.-Q.; Huang, Z.-S. *Eur. J. Med. Chem.* **2015**, *92*, 540.
17. Nitiss, J. L. *Nat. Rev. Cancer* **2009**, *9*, 327.
18. Liang, F.; Wan, S. H.; Li, Z.; Xiong, X. Q.; Yang, L.; Zhou, X.; Wu, C. T. *Curr. Med. Chem.* **2006**, *13*, 711.
19. Liang, X. Y.; Sadler, P. J. *Chem. Soc. Rev.* **2004**, *33*, 246.
20. Cabbiness, D. K.; Margerum, D. W. *J. Am. Chem. Soc.* **1969**, *91*, 6540.
21. Khan, A.; Nicholson, G.; Greenman, J.; Madden, L.; McRobbie, G.; Pannecouque, C.; De Clercq, E.; Ullom, R.; Maples, D. L.; Maples, R. D.; Silversides, J. D.; Hubin, T. J.; Archibald, S. J. *J. Am. Chem. Soc.* **2009**, *131*, 3416.
22. Haas, K. L.; Franz, K. J. *Chem. Rev.* **2009**, *109*, 4921.
23. Sibert, J. W.; Cory, A. H.; Cory, J. G. *Chem. Commun.* **2002**, 154.
24. Saudan, C.; Ceroni, P.; Vicinelli, V.; Balzani, V.; Gorka, M.; Lee, S. K.; Vogtle, F.; Orlandi, M.; Bartolini, G.; Tavolari, S.; Rocchi, P.; Ferreri, A. M. *Supramol. Chem.* **2004**, *16*, 541.
25. Brana, M. F.; Ramos, A. *Curr. Med. Chem.: Anti-Cancer Agents* **2001**, *1*, 237.
26. Stone, R. M.; Mazzola, E.; Neuberg, D.; Allen, S. L.; Pigneux, A.; Stuart, R. K.; Wetzler, M.; Rizzieri, D.; Erba, H. P.; Damon, L.; Jang, J. H.; Tallman, M. S.; Warzocha, K.; Masszi, T.; Sekeres, M. A.; Egyed, M.; Horst, H. A.; Selleslag, D.; Solomon, S. R.; Venugopal, P.; Lundberg, A. S.; Powell, B. *J. Clin. Oncol.: Official J. Am. Soc. Clin. Oncol.* **2015**, *33*, 1252.